<Electronic Supplementary Information>

Recyclable scavengers for photo-cyclopropanation via *in situ* crystallization process

Haeri Lee, Eunkyung Choi, Tae Hwan Noh and Ok-Sang Jung*

Department of Chemistry and Chemistry Institute for Functional Materials, Pusan National University, Busan 46241, Korea.

*e-mail: oksjung@pusan.ac.kr

Refinement details of structures with the SQUEEZE routine in PLATON.

For **1**$(Cl)_6$, **2**$\cdot(NO_3)_6$, and **3**$\cdot(NO_3)_6$, solvate molecules in the voids were highly disordered. For **2**$\cdot(I_3)_3\cdot(NO_3)_3$, solvate molecules and anions were highly disordered in a large volume. Those were impossible to refine using conventional discrete-atom models. The residual electron density was treated as diffuse contributions using the SQUEEZE of the PLATON software and located a series of voids (see below).[1]

For **1**$(Cl)_6$

_refine_special_details

The structure contains large solvent accessible voids. SQUEEZE procedure has been used in order to remove electronic density peaks from solvent molecules. According to the TGA and proton NMR spectra, the asymmetric unit of **1**$(Cl)_6$ may contains two methanol molecules.

```
loop_
 _platon_squeeze_void_nr
 _platon_squeeze_void_average_x
 _platon_squeeze_void_average_y
 _platon_squeeze_void_average_z
 _platon_squeeze_void_volume
 _platon_squeeze_void_count_electrons
 _platon_squeeze_void_content
  1  0.333  0.667  0.020      317      120 ' '
  2  0.667  0.333  0.187      326      120 ' '
  3  0.000  0.000  0.354      323      119 ' '
  4  0.333  0.667  0.520      318      120 ' '
  5  0.667  0.333  0.687      326      120 ' '
  6  0.000  0.000  0.854      323      119 ' '
_platon_squeeze_void_probe_radius          1.20
_platon_squeeze_details                    ?
```

For **2**·$(NO_3)_6$,

_refine_special_details

The structure contains large solvent accessible voids. According to the TGA and proton NMR spectra, the asymmetric unit of **2**·$(NO_3)_6$ contains about five dimethyl sulfoxide and six water molecules. Except refined five dimethyl sulfoxide, SQUEEZE procedure has been used in order to remove electronic density peaks from disordered solvent molecules.

```
loop_
 _platon_squeeze_void_nr
 _platon_squeeze_void_average_x
 _platon_squeeze_void_average_y
 _platon_squeeze_void_average_z
 _platon_squeeze_void_volume
 _platon_squeeze_void_count_electrons
 _platon_squeeze_void_content
  1  0.000  0.431  0.250      699      266 ' '
  2  0.000  0.569  0.750      701      266 ' '
  3  0.500  0.069  0.750      701      266 ' '
  4  0.500  0.931  0.250      699      266 ' '
_platon_squeeze_void_probe_radius              1.20
_platon_squeeze_details                        ?
```

For **2**·$(I_3)_3$·$(NO_3)_3$,

_refine_special_details

According to EDX and HR-ESI-MS data, the CCDC-1453026 crystals consist of **2**·$(I_3)_3$·$(NO_3)_3$ composition. Whereas all three triiodide anions were fully refined, three nitrate anions were highly disordered on account of crystal's low stability during X-ray data collection. Additionally, the structure contains large solvent accessible voids. SQUEEZE procedure has been used in order to remove electronic density peaks. According to the TGA and proton NMR spectra, the asymmetric unit of **2**·$(I_3)_3$·$(NO_3)_3$ may contains five chloroform molecules.

```
loop_
```

_platon_squeeze_void_nr
_platon_squeeze_void_average_x
_platon_squeeze_void_average_y
_platon_squeeze_void_average_z
_platon_squeeze_void_volume
_platon_squeeze_void_count_electrons
_platon_squeeze_void_content
1 0.000 0.000 -0.010 2243 928 ' '
2 0.750 0.250 0.000 344 110 ' '
3 0.509 0.500 0.014 2243 928 ' '
4 1.250 0.750 0.000 344 110 ' '
5 0.028 0.142 0.183 7 0 ' '
6 0.528 0.642 0.183 7 0 ' '
7 0.944 0.294 0.217 6 1 ' '
8 0.444 0.794 0.217 6 1 ' '
9 0.056 0.294 0.283 6 1 ' '
10 0.556 0.794 0.283 6 1 ' '
11 0.972 0.142 0.317 7 0 ' '
12 0.472 0.642 0.317 7 0 ' '
13 0.250 0.250 0.500 344 110 ' '
14 0.750 0.750 0.500 344 110 ' '
15 0.528 0.358 0.683 7 0 ' '
16 0.028 0.858 0.683 7 0 ' '
17 0.444 0.206 0.717 6 1 ' '
18 0.944 0.706 0.717 6 1 ' '
19 0.556 0.206 0.783 6 1 ' '
20 0.056 0.706 0.783 6 1 ' '
21 0.472 0.358 0.817 7 0 ' '
22 0.972 0.858 0.817 7 0 ' '
_platon_squeeze_void_probe_radius 1.20
_platon_squeeze_details ?

For **3**·$(NO_3)_6$,

_refine_special_details

The structure contains large solvent accessible voids. According to the TGA and proton NMR spectra, the asymmetric unit of **3**·$(NO_3)_6$ contains about twelve dimethyl sulfoxide and four water molecules. Except refined six dimethyl sulfoxide, SQUEEZE procedure has been used in order to remove electronic density peaks from disordered solvent molecules.

```
loop_
 _platon_squeeze_void_nr
 _platon_squeeze_void_average_x
 _platon_squeeze_void_average_y
 _platon_squeeze_void_average_z
 _platon_squeeze_void_volume
 _platon_squeeze_void_count_electrons
 _platon_squeeze_void_content
  1  0.528  0.250 -0.008      2502       870 ' '
  2  1.000  0.500  0.000       323        86 ' '
  3  0.472  0.750  0.006      2501       869 ' '
  4  0.404 -0.002  0.049        11         0 ' '
  5  1.000  1.000  0.500       323        86 ' '
  6  0.596  0.498  0.451        11         1 ' '
  7  0.404  0.502  0.549        11         0 ' '
  8  0.596  0.002  0.951        11         1 ' '
_platon_squeeze_void_probe_radius          1.20
_platon_squeeze_details                    ?
```

■ References

1. A. L. Spek, *Acta Cryst.*, 2015, **C71**, 9–18.

Table S1 Crystal data and refinement parameters for **1**$(Cl)_6$, **1**$(NO_3)_6$, **2**$\cdot(NO_3)$, **2**$\cdot(I_3)_3\cdot(NO_3)_3$, **3**$\cdot(NO_3)_6$, and **4**$\cdot(NO_3)_6$.

	1$(Cl)_6$	**1**$(NO_3)_6$	**2**$\cdot(NO_3)_6$	**2**$\cdot(I_3)_3\cdot(NO_3)_3$	**3**$\cdot(NO_3)_6$	**4**$\cdot(NO_3)_6$
Formula	$C_{66}H_{78}Cl_6N_6O_{18}Pd_3$	$C_{66}H_{72}N_{12}O_{33}Pd_3S_3$	$C_{146}H_{204}N_{18}O_{64}Pd_3S_{10}$	$C_{136}H_{130}Cl_{30}I_9N_{15}O_{33}Pd_3$	$C_{138}H_{200}N_{30}O_{52}Pd_3S_{12}$	$C_{111}H_{187.42}N_{36}O_{63.71}Pd_3$
M_w	1775.24	1976.73	3875.06	5027.34	3815.19	3364.94
Crystal system	Trigonal	Trigonal	Monoclinic	Monoclinic	Monoclinic	Monoclinic
Space group	*R*3*c*	*R*3*c*	*C*2/*c*	*C*2/*c*	$P2_1/c$	$P2_1/c$
a (Å)	24.927(2)	25.4354(4)	21.8830(7)	14.029(3)	18.3794(5)	16.3485(2)
b (Å)			36.7927(7)	41.786(8)	72.214(3)	27.8059(3)
c (Å)	19.707(3)	21.3755(6)	24.3223(6)	37.004(6)	15.4212(5)	33.4695(4)
β (°)			105.571(2)	94.315(9)	110.993(2)	96.134(1)
V (Å^3)	10604(2)	11976.3(5)	18864.0(9)	21631(7)	19117(1)	15127.6(3)
Z	6	6	4	4	4	4
ρ (g cm^{-3})	1.668	1.644	1.364	1.544	1.326	1.477
μ (mm^{-1})	1.056	0.841	0.480	1.960	0.491	0.456
R_{int}	0.1789	0.0687	0.0468	0.1051	0.0758	0.0569
GoF on F^2	1.050	1.036	1.083	1.036	1.029	1.014
R_1 [$I>2\sigma(I)$][a]	0.0891	0.0595	0.0644	0.1314	0.1288	0.0785
wR_2 (all data)[b]	0.1644	0.1672	0.1974	0.4415	0.3732	0.2596
Completeness (%)	100.0	100.0	100.0	99.9	74.8	100.0

[a] $R_1 = \Sigma||F_o| - |F_c||/\Sigma|F_o|$, [b] $wR_2 = (\Sigma[w(F_o^2 - F_c^2)^2]/\Sigma[w(F_o^2)^2])^{1/2}$

Table S2 Selected bond length and angles of **1**$(Cl)_6$, **1**$(NO_3)_6$, **2**$\cdot(NO_3)$, **2**$\cdot(I_3)_3\cdot(NO_3)_3$, **3**$\cdot(NO_3)_6$, and **4**$\cdot(NO_3)_6$.

1$(Cl)_6$		**1**$(NO_3)_6$		**2**$\cdot(NO_3)_6$		**2**$\cdot(I_3)_3\cdot(NO_3)_3$	
Pd(1)–N(1)	1.99(1)	Pd(1)–N(1)	2.031(9)	Pd(1)–N(1)	2.045(4)	Pd(1)–N(1)	2.07(1)
Pd(1)–N(2)	2.03(1)	Pd(1)–N(2)	2.02(1)	Pd(1)–N(4)	2.016(4)	Pd(1)–N(3)$^{\#2}$	2.07(1)
Pd(1)–Cl(1)	2.282(5)	Pd(1)–O(5)	1.99(1)	Pd(1)–N(3)$^{\#1}$	2.041(4)	Pd(1)–N(4)	2.00(1)
Pd(1)–Cl(2)	2.314(5)	Pd(1)–O(8)	2.02(1)	Pd(1)–N(6)$^{\#1}$	2.024(4)	Pd(1)–N(6)$^{\#2}$	2.08(1)
				Pd(2)–N(2)	2.044(3)	Pd(2)–N(2)	2.00(2)
				Pd(2)–N(2)$^{\#1}$	2.044(3)	Pd(2)–N(5)	2.03(2)
				Pd(2)–N(5)	2.034(3)		
N(1)–Pd(1)–N(2)	176.4(6)	N(1)–Pd(1)–N(2)	178.4(3)	Pd(2)–N(5)$^{\#1}$	2.034(3)	N(1)–Pd(1)–N(3)$^{\#2}$	173.6(4)
N(1)–Pd(1)–Cl(1)	87.0(4)	N(1)–Pd(1)–O(5)	86.8(5)			N(1)–Pd(1)–N(4)	90.4(4)
N(1)–Pd(1)–Cl(2)	90.5(4)	N(1)–Pd(1)–O(8)	89.9(4)	N(1)–Pd(1)–N(4)	87.9(2)	N(1)–Pd(1)–N(6)$^{\#2}$	90.1(5)
N(2)–Pd(1)–Cl(1)	93.6(4)	N(2)–Pd(1)–O(5)	92.7(4)	N(1)–Pd(1)–N(3)$^{\#1}$	173.0(1)	N(3)$^{\#2}$–Pd(1)–N(6)$^{\#2}$	92.1(5)
N(2)–Pd(1)–Cl(2)	171.7(2)	N(2)–Pd(1)–O(8)	90.6(4)	N(1)–Pd(1)–N(6)$^{\#1}$	94.0(2)	N(4)–Pd(1)–N(6)$^{\#2}$	175.4(5)
		O(5)–Pd(1)–O(8)	176.7(5)	N(3)$^{\#1}$–Pd(1)–N(6)$^{\#1}$	87.9(2)	N(2)–Pd(2)–N(2)$^{\#2}$	175.8(8)
				N(2)–Pd(2)–N(5)	86.9(1)	N(2)–Pd(2)–N(5)	91.8(7)
				N(5)–Pd(2)–N(5)$^{\#1}$	174.5(2)	N(2)$^{\#2}$–Pd(2)–N(5)	88.1(7)

3$\cdot(NO_3)_6$		**4**$\cdot(NO_3)_6$	
Pd(1)–N(1)	2.01(1)	Pd(1)–N(1)	2.027(5)
Pd(1)–N(4)	2.06(1)	Pd(1)–N(4)	2.001(5)
Pd(1)–N(7)	2.031(9)	Pd(1)–N(13)	2.020(5)
Pd(1)–N(16)	2.04(1)	Pd(1)–N(22)	2.023(5)
Pd(2)–N(2)	2.01(1)	Pd(2)– N(2)	2.033(5)
Pd(2)–N(5)	2.02(1)	Pd(2)–N(10)	2.009(5)
Pd(2)–N(10)	2.01(1)	Pd(2)–N(16)	2.019(5)
Pd(2)–N(19)	1.99(1)	Pd(2)–N(25)	2.013(5)
Pd(3)–N(3)	2.02(1)	Pd(3)–N(3)	2.032(5)
Pd(3)–N(6)	2.08(1)	Pd(3)–N(7)	2.011(6)
Pd(3)–N(13)	1.96(1)	Pd(3)–N(19)	1.999(6)
Pd(3)–N(22)	1.99(1)	Pd(3)–N(28)	2.009(6)
N(1)–Pd(1)–N(4)	175.5(4)	N(1)–Pd(1)–N(4)	176.8(2)
N(1)–Pd(1)–N(7)	88.7(4)	N(1)–Pd(1)–N(13)	89.5(2)
N(4)–Pd(1)–N(7)	91.4(4)	N(1)–Pd(1)–N(22)	92.3(2)
N(7)–Pd(1)–N(16)	178.3(3)	N(4)–Pd(1)–N(13)	90.8(2)
N(2)–Pd(2)–N(5)	173.1(5)	N(13)–Pd(1)–N(22)	177.1(2)
N(5)–Pd(2)–N(10)	91.9(5)	N(2)–Pd(2)–N(10)	175.6(2)
N(5)–Pd(2)–N(19)	86.5(5)	N(2)–Pd(2)–N(16)	91.8(2)
N(10)–Pd(2)–N(19)	177.5(5)	N(2)–Pd(2)–N(25)	89.1(2)
N(3)–Pd(3)–N(6)	176.2(5)	N(10)–Pd(2)–N(16)	90.9(2)
N(3)–Pd(3)–N(13)	88.9(5)	N(16)–Pd(2)–N(25)	178.5(2)
N(6)–Pd(3)–N(13)	89.5(5)	N(3)–Pd(3)–N(7)	178.6(2)
N(13)–Pd(3)–N(22)	177.5(6)	N(3)–Pd(3)–N(19)	89.4(2)
		N(3)–Pd(3)–N(28)	91.6(2)
		N(7)–Pd(3)–N(19)	91.9(3)
		N(19)–Pd(3)–N(28)	175.7(3)

$^{\#1}$ -x,y,-z+3/2; $^{\#2}$ -x+1,y,-z+1/2

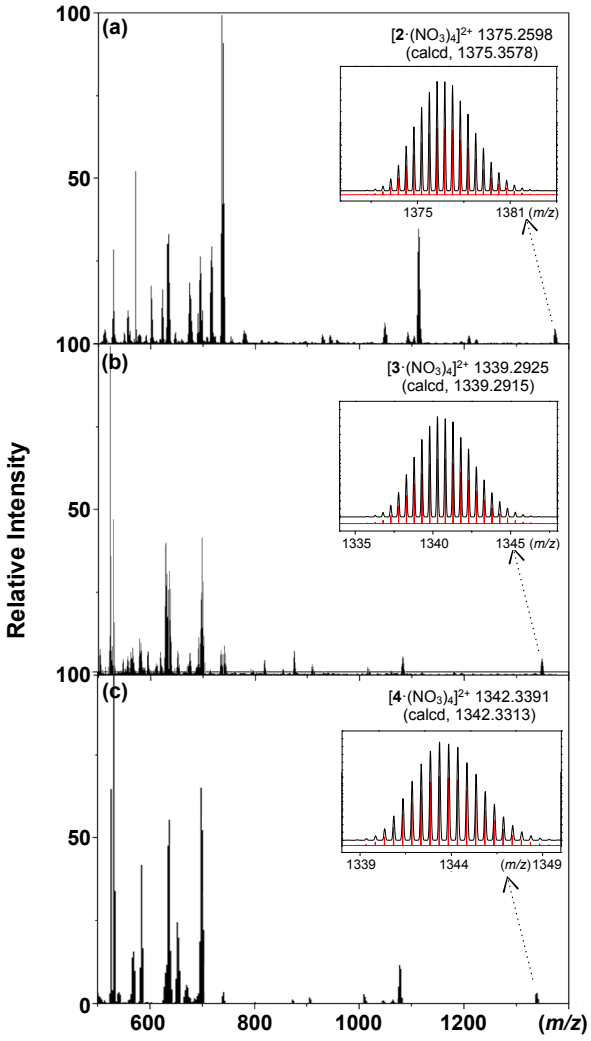

Fig. S1 High resolution-ESI-TOF-mass data of **2**·$(NO_3)_6$ (a), **3**·$(NO_3)_6$ (b), and **4**·$(NO_3)_6$ (c). Insets show the magnified data of calculated (red) and experimental mass peaks (black) corresponding to [**2**·$(NO_3)_6 - 2NO_3^-]^{2+}$, [**3**·$(NO_3)_6 - 2NO_3^-]^{2+}$, and [**4**·$(NO_3)_6 - 2NO_3^-]^{2+}$, respectively.

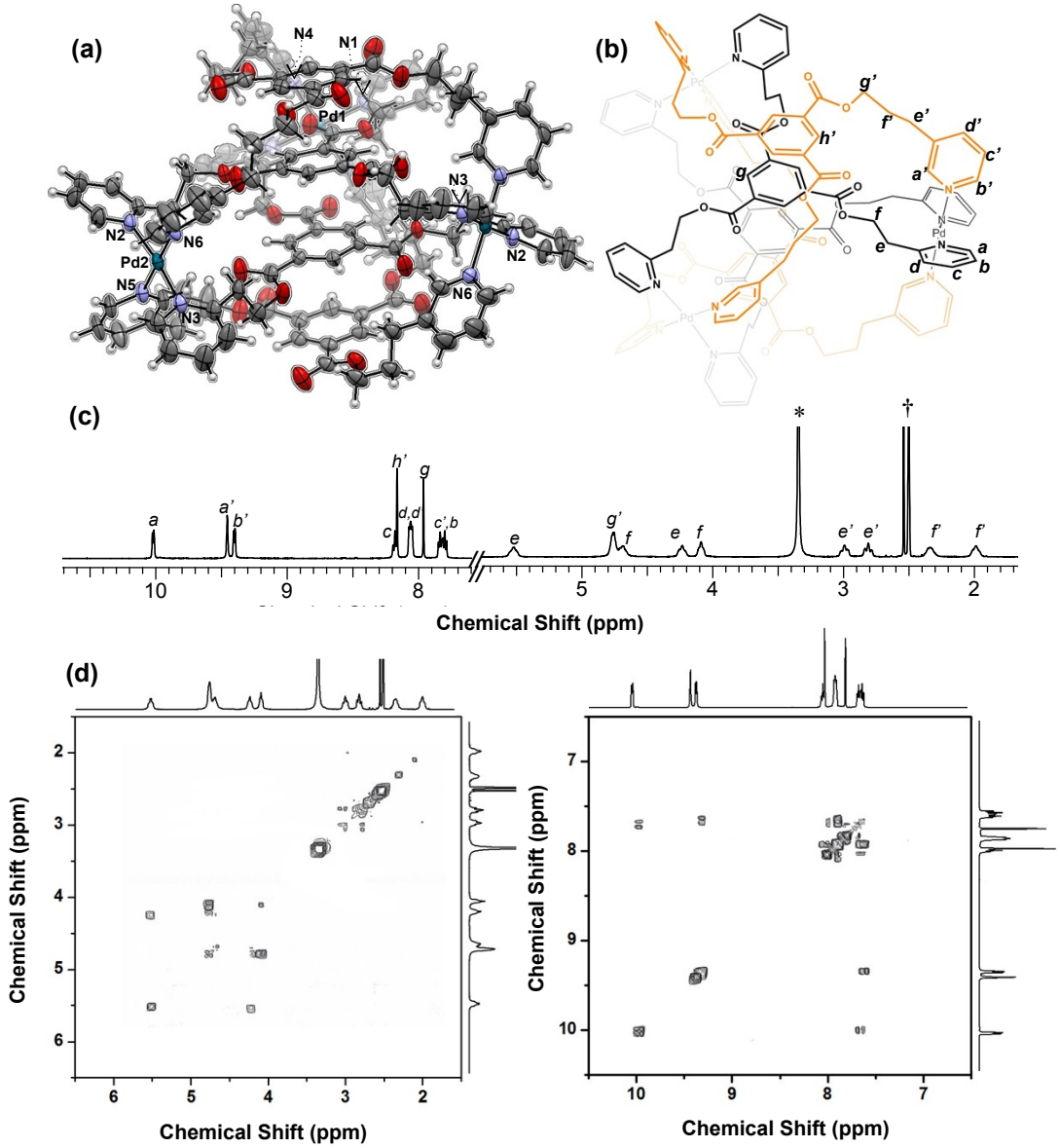

Fig. S2 ORTEP drawing of **2**·$(NO_3)_6$ showing thermal ellipsoids at 50 % probability (a), proton assignment (b), ^{1}H NMR (c), and ^{1}H-^{1}H COSY NMR spectra (d) of **2**·$(NO_3)_2$ in Me_2SO-d_6 (*, HOD; dagger, Me_2SO and CHD_2CD_3SO).

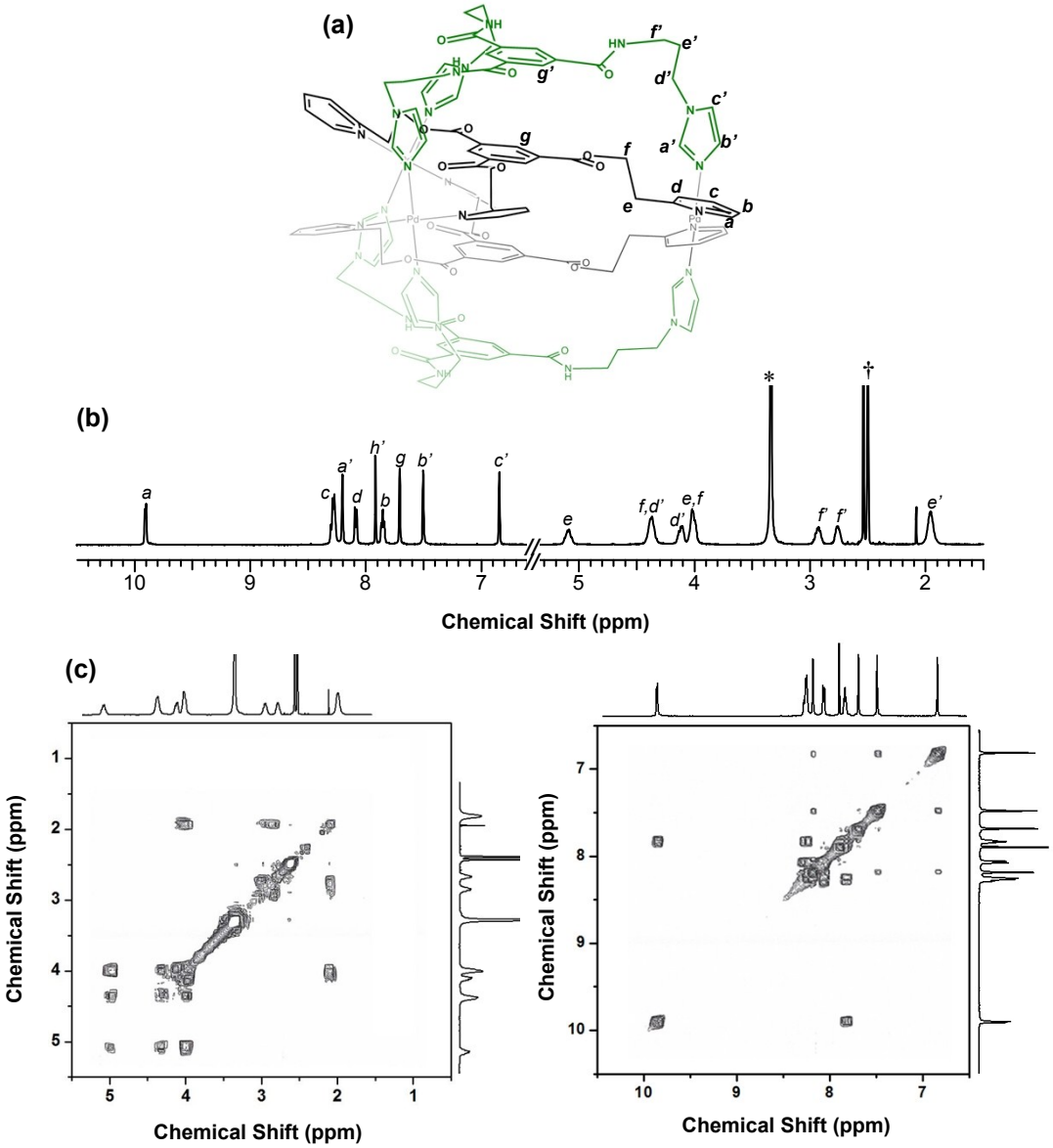

Fig. S3 Proton assignment (a), ^{1}H NMR (b), and ^{1}H-^{1}H COSY NMR (c) spectra of **3**·$(NO_3)_2$ in Me_2SO-d_6 (*, HOD; dagger, Me_2SO and CHD_2CD_3SO).

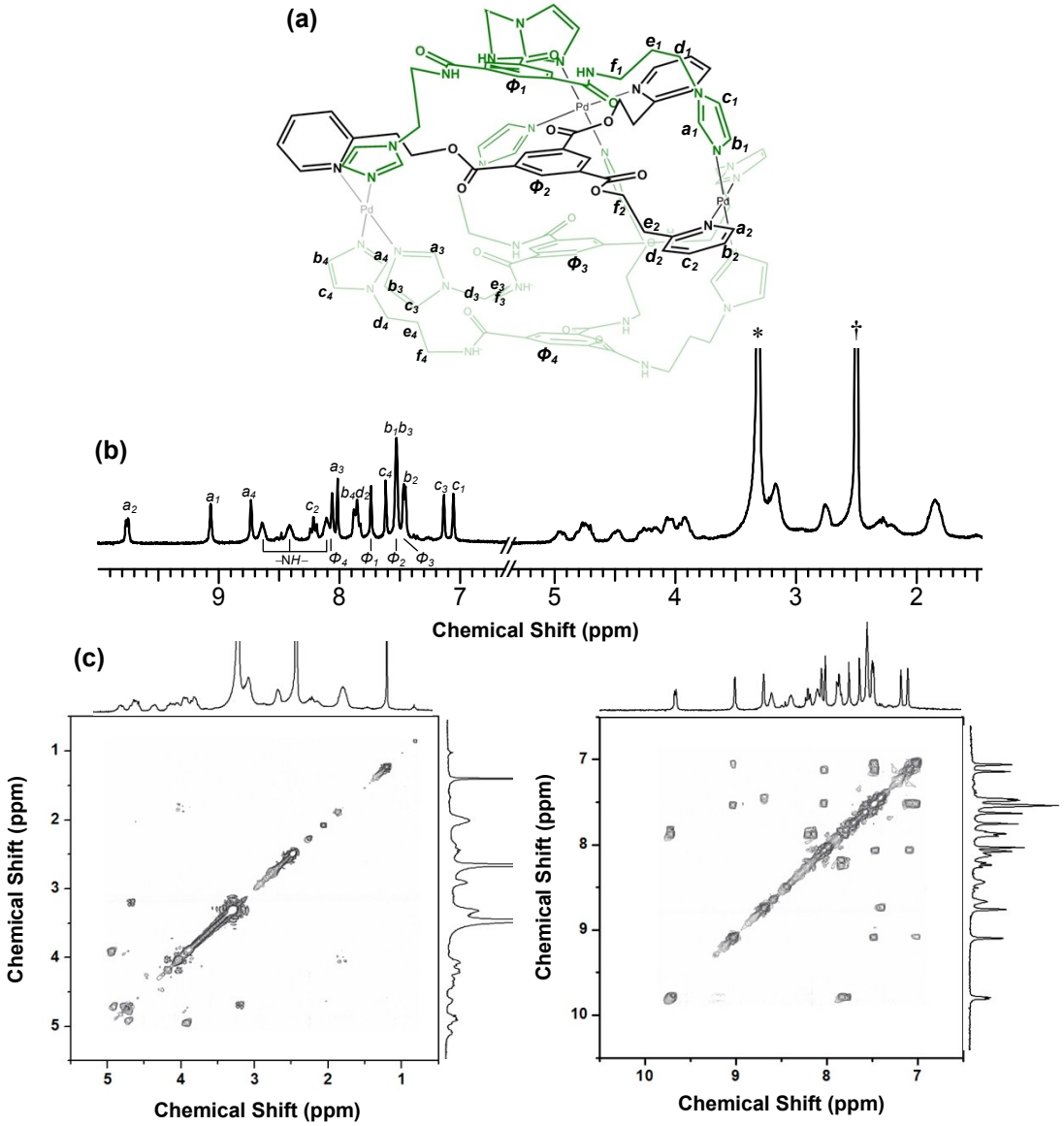

Fig. S4 Proton assignment (a), ^{1}H NMR (b), and ^{1}H-^{1}H COSY NMR (c) spectra of **4**·$(NO_3)_2$ in Me_2SO-d_6 (*, HOD; dagger, Me_2SO and CHD_2CD_3SO).

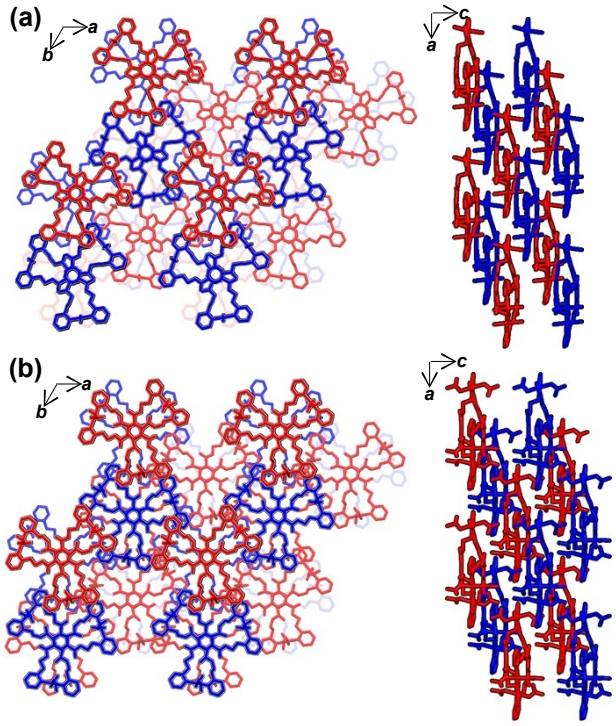

Fig. S5 Top (left) and side (right) views of packing structures of 2-layered tripalladium(II)cyclophanes, **1**$(Cl)_6$ (a), and **1**$(NO_3)_6$ (b). Anions, hydrogen atoms, and solvate molecules were omitted for clarity.

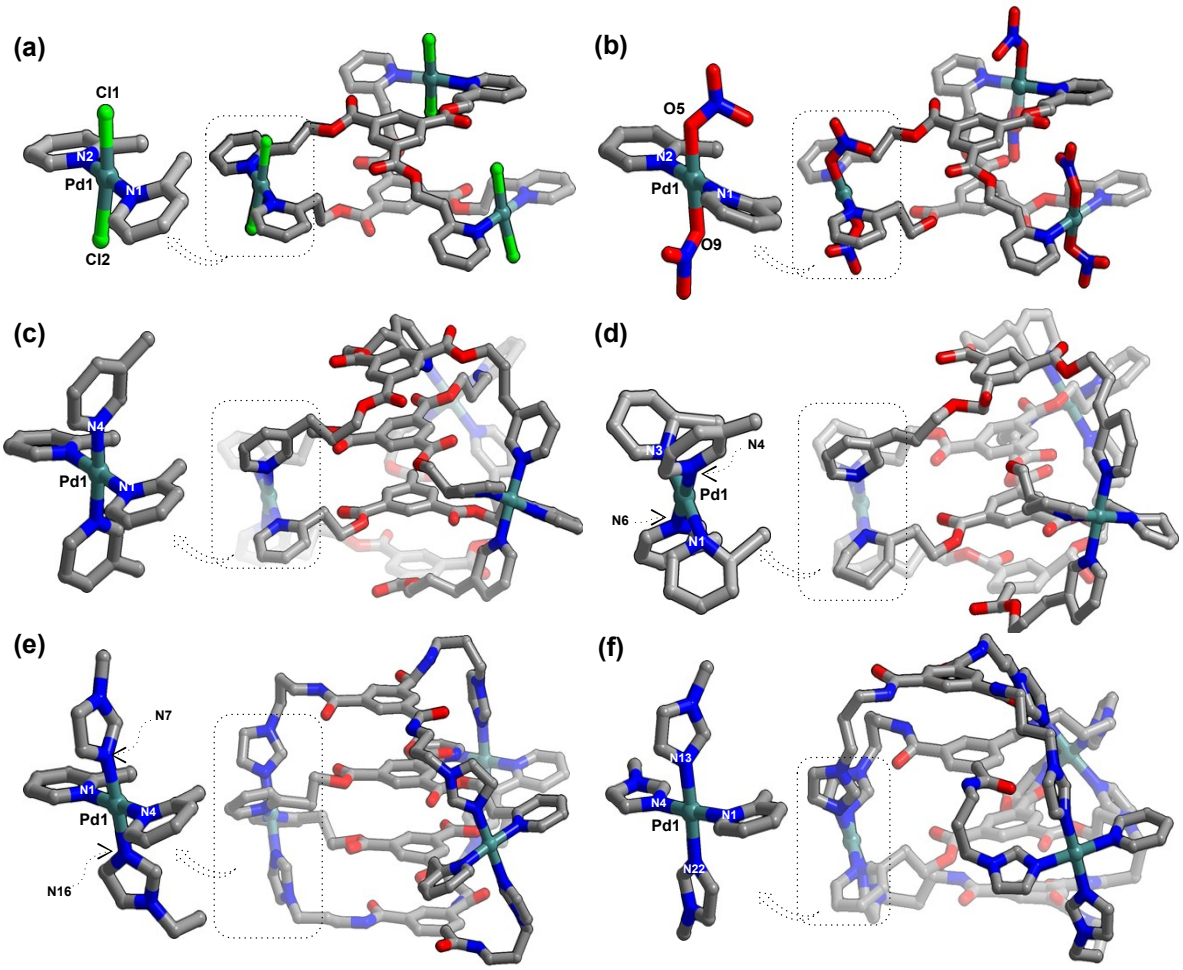

Fig. S6 The coordination geometry of palladium(II) center in the tripalladium(II)cyclophane molecules, **1**$(Cl)_6$ (a), **1**$(NO_3)_6$ (b), **2**$\cdot(NO_3)_6$ (c), **2**$\cdot(I_3)_3\cdot(NO_3)_3$ (d), **3**$\cdot(NO_3)_6$ (e), and **4**$\cdot(NO_3)_6$ (f). Anions, hydrogen atoms, and solvate molecules were omitted for clarity.

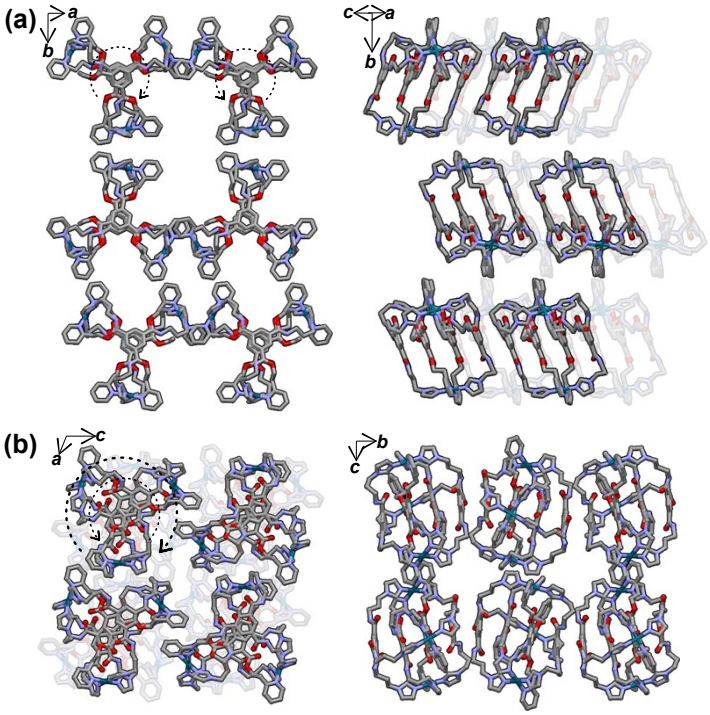

Fig. S7 Top (left) and side (right) views of columnar packed structures of 4-layered tripalladium(II)cyclophanes, **3**·$(NO_3)_6$ (a), and **4**·$(NO_3)_6$ (b). Anions, hydrogen atoms, and solvate molecules were omitted for clarity.

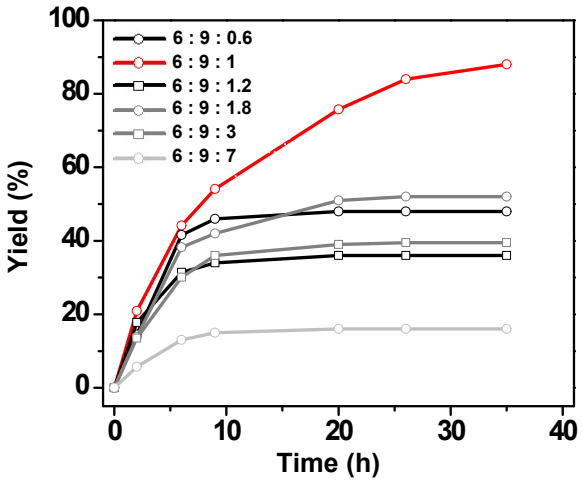

Fig. S8 Reaction yields versus the time for photo-cyclopropanation of 1-methylcyclohexene with **2**·$(NO_3)_6$ depending on the mole ratios in $CDCl_3$ at 350 nm UV radiation.

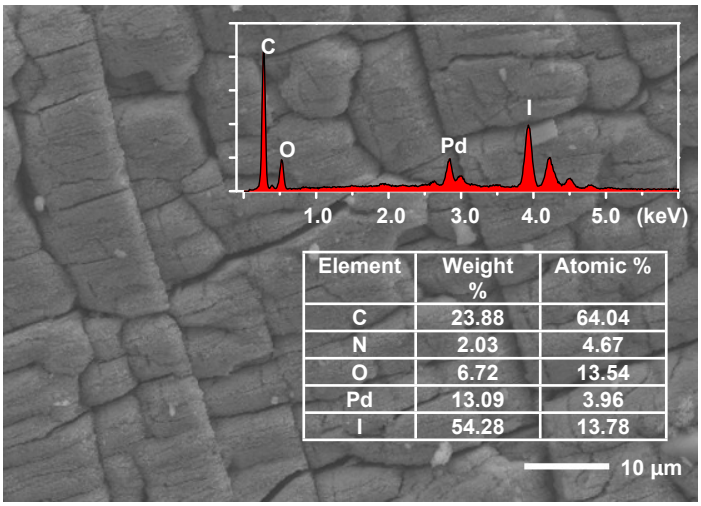

Element	Weight %	Atomic %
C	23.88	64.04
N	2.03	4.67
O	6.72	13.54
Pd	13.09	3.96
I	54.28	13.78

Fig. S9 SEM image and EDX data of **2**·$(I_3)_3$·$(NO_3)_3$ crystal.

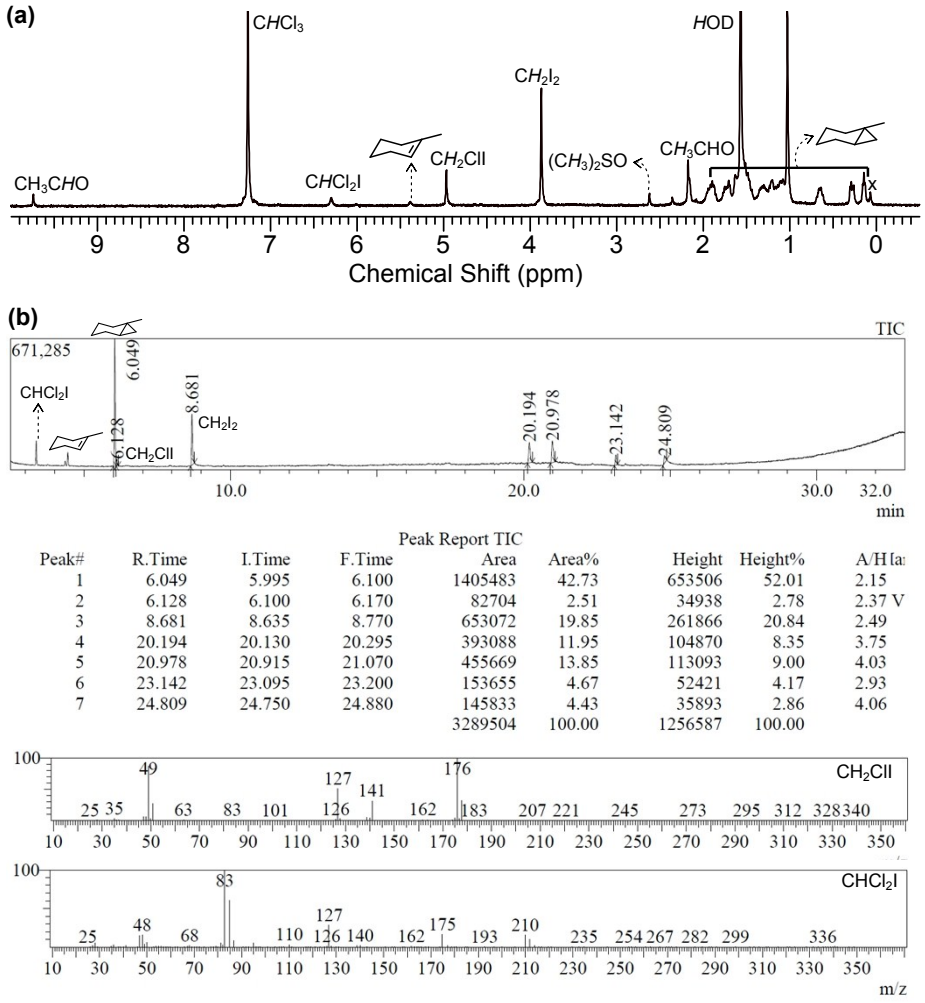

Fig. S10 ^{1}H NMR spectrum in $CDCl_3$ (a) and gas chromatography mass analysis (b) distilled photo-reaction solution. Inset spectrums show the spectra of CH_2ClI (ret. time, 3.422 min) and $CHCl_2I$ (ret. time, 6.128 min).

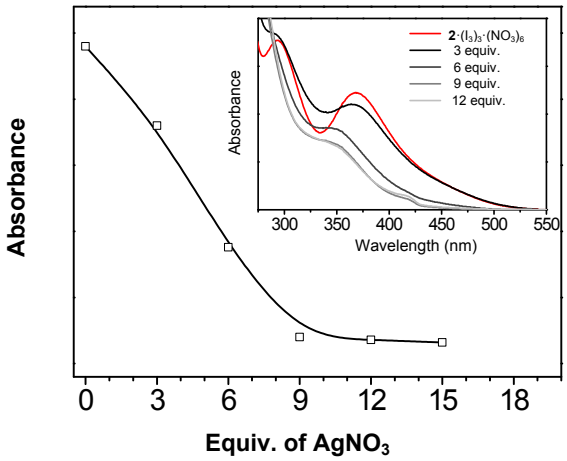

Fig. S11 Plot of the absorbance of λ_{max} *versus* the amount of $AgNO_3$ for anion exchange of **2**·$(I_3)_3$·$(NO_3)_3$ in a mixed solution of H_2O and Me_2SO (*v*/*v* = 19 : 1). Inset shows UV-Vis absorption spectra in accordance with the added amount of $AgNO_3$.

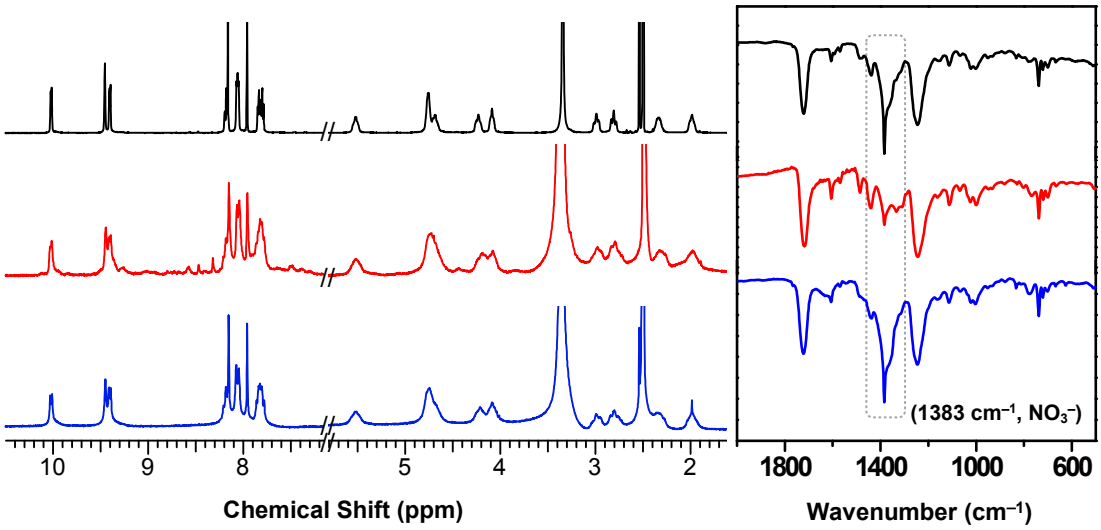

Fig. S12 ^{1}H NMR and IR spectra of **2**·$(NO_3)_6$ (black), **2**·$(I_3)_3$·$(NO_3)_3$ (red), and recovered **2**·$(NO_3)_6$ (blue). See Figure S2 in the Supporting Information for the assignments in part (b).

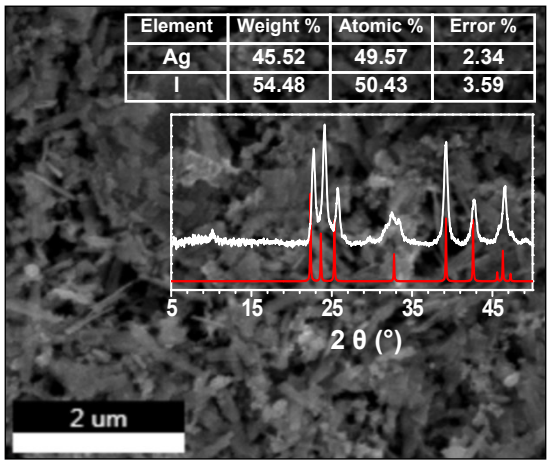

Fig. S13 SEM image of the residue obtained during anion exchange of **2**·$(I_3)_3$·$(NO_3)_3$ with $AgNO_3$. Inset shows EDX analysis and powder X-ray diffraction pattern for AgI residue (white line). Red line represents the reference pattern of AgI (space group *P*63*mc*, JCPDS card no. 3-0940).